Available online at www.sciencedirect.com
SCIENCE DIRECT®
Computer Physics Communications 169 (2005) 353–361
Computer Physics Communications
www.elsevier.com/locate/cpc

Simulating astrophysical phenomena: challenges and achievements

Ewald Müller

Max-Planck-Institut für Astrophysik, Karl-Schwarzschild-Str.1, D-85748 Garching, Germany

Available online 9 April 2005

Abstract

Simulation is an indispensable and expedient tool for understanding many astrophysical phenomena. Addressing a few challenging computational problems in astrophysics, it is illustrated that simulation can provide the link between observations and theoretical models of astrophysical phenomenon. For obvious reasons, the discussion is restricted to a few specific timely problems, the main bias being the personal involvement of the author into the simulation of these astrophysics problems. In particular, recent work on core collapse supernovae and their gravitational wave signal, on extragalactic jets, and on the modeling of gamma-ray burst sources is presented.

PACS: 04.30.Db; 47.11.+j; 97.60.Bw; 98.62.Nx; 98.70.Rz

Keywords: Gravitational waves; Computational methods in fluid dynamics; Supernovae; Jets and bursts; Gamma-ray bursts

1. Introduction

In astrophysics one is in the extraordinary situation, that the objects of interest (e.g., stars or galaxies) are not accessible to any kind of manipulation. No experiments can be performed, and observations of a particular one-time event (e.g., of a specific supernova) cannot be repeated. Hence, astrophysicists have to rely solely on the information they can receive from astrophysical phenomena via electromagnetic radiation, particle radiation, like, e.g., neutrinos or cosmic rays, and gravitational radiation.

The situation is further complicated by the fact that physical processes giving rise to the astrophysical phenomenon may occur deep inside the observed object, i.e. we only have indirect evidence of these processes. This is the case, for example, in a core collapse supernova explosion where the explosion of the star is triggered by the gravitational collapse of its iron core in a fraction of a second while the observable (electromagnetic) supernova explosion only begins hours later. Moreover, the processes one tries to understand often occur on time scales long compared to the human life span, i.e. one is stuck with a snapshot of the phenomena. This holds for extragalactic jets, which are collimated flow structures emanating from active galactic nuclei and extending up to several hundred

E-mail address: emueller@mpa-garching.mpg.de (E. Müller).

0010-4655/$ – see front matter
doi:10.1016/j.cpc.2005.03.079

thousands of light years into intergalactic space. The inferred time scale for the formation of these jets is several million years.

Under the circumstances one constructs a theoretical model which incorporates all the physical processes thought to be of importance for the astrophysical phenomenon, and which in almost all cases involves some degrees of freedom manifesting themselves as parameters of the model. The model, if of any value at all, should make some definite predictions about the properties or behavior of the object or phenomenon. In order to compute these predictions one requires simulation, because elaborated models consist of a set of nonlinear structure equations or evolutionary equations. Comparing the model predictions with observations allows one to constrain the parameters of the model, or to verify or falsify certain model assumptions. In the latter case, one can try to improve or modify the model to achieve a better agreement with the observation, and start the procedure all over again. Thus, simulation provides the link between theory and observation in the iterative process to understand observed astrophysical phenomena.

2. Simulations of core collapse supernovae

Supernova explosions are either powered by the gravitational binding energy released during the collapse of a stellar core to a neutron star (SNe II, Ib and Ic; [1]) or a black hole, or by the energy released during explosive burning of degenerate thermonuclear fuel (SNe Ia; [2]).

Theoretical and numerical models of core collapse SNe are based on the idea, that the implosion of the iron core of a massive main sequence star $M \gtrsim 9M_\odot$ ($M_\odot$ is the solar mass) at the end of its thermonuclear evolution causes a supernova explosion with violent mass ejection ($v_{\rm eject} \sim 10^4$ km/sec) and the formation of a compact remnant, i.e. a neutron star or a black hole (for a review, see, e.g., [3]). The energy source for the explosion is the gravitational binding energy of the forming neutron star, which is of the order $E_{\rm b} \sim 3 \times 10^{53} (M/M_\odot)^2 (R/10\ {\rm km})^{-1}$ erg, where M and R are the mass and the radius of the neutron star, respectively. As predicted by theoretical models and as proven through observations of SN 1987A, the overwhelming fraction of the binding energy (about 99%) is carried away by neutrinos. Roughly 1% of the binding energy is transfered into kinetic energy ($\sim 10^{51}$ erg) of the ejecta, and only about 10^{-4} of the liberated energy is emitted in form of electromagnetic radiation ($\sim 10^{49}$ erg).

At the end of the final thermonuclear burning stage of a massive star (i.e. after Si-core burning) the electron fraction (per baryon) in the stellar core which then consists mainly of iron group nuclei (hence iron core) is $0.42 \lesssim Y_{\rm e} \lesssim 0.44$, because of electron captures which occurred during previous oxygen and core silicon burning. The central density and temperature are $\varrho_{\rm c} \sim 10^{10}\ {\rm g\,cm^{-3}}$ and $T_{\rm c} \sim (8\text{–}10) \times 10^9$ K, respectively. Hence, the iron core is predominantly supported against gravity by the pressure of its degenerate relativistic electrons, i.e. it is gravitationally stable as long as its mass does not exceed the Chandrasekhar mass $M_{\rm Ch} = 1.457 (2Y_{\rm e})^2 M_\odot$ [4]. However, this critical value is eventually exceeded, because (i) the core mass grows as a result of Si-shell burning, (ii) electron captures further reduce $Y_{\rm e}$, and (iii) the thermal pressure in the core is reduced due to (endothermic) photo-disintegration of nuclei by energetic photons.

The core suffers a dynamic collapse ($\tau_{\rm coll} \sim 0.1$ s) until the central density exceeds that of nuclear matter ($\sim 2 \times 10^{14}\ {\rm g\,cm^{-3}}$). The incompressibility of nuclear matter eventually halts and then reverses the collapse. As a consequence of this bounce a hydrodynamic shock wave forms which propagates outwards into the still infalling outer parts of the iron core. Numerical simulations and analytical estimates show that the initial energy of the shock wave is of the order of $E_{\rm sh}^{\rm (i)} \sim (4\text{–}10) \times 10^{51}$ erg much more than is required to explain the observed (kinetic and electromagnetic) energy output of a core collapse supernova. However, while propagating outward the shock wave is severely damped by photo-disintegration of heavy nuclei into free nucleons the energy loss being of the order $E_{\rm loss} \sim 1.6 \times 10^{51}\ {\rm erg}/0.1 M_\odot$. Hence, the shock eventually stalls and turns into an accretion shock, i.e. no *prompt* supernova explosion results.

Initially neutrinos can leak out of the core during the collapse, because the density and hence the opacity of core matter is relatively low. The leakage of neutrinos results in a deleptonization of the core, i.e. $Y_{\rm e}$ decreases. For densities $\varrho \gtrsim 3 \times 10^{12}\ {\rm g\,cm^{-3}}$ the neutrino diffusion time scale $\tau_{\rm diff} > \tau_{\rm coll}$, which implies that the total lepton number $Y_{\rm L} = Y_{\rm e} + Y_\nu$ is

constant during further collapse. This epoch of the collapse is called *neutrino trapping*. In analogy to photons a neutrinosphere can be defined as the surface, where the optical depth is in the range $2/3 \lesssim \tau \leqslant 1$. Deleptonization neutrinos as well as neutrino anti-neutrino pairs of all flavors copiously produced by thermal processes deposit energy in the layers between the neutrinosphere and the stalled prompt supernova shock during a period of a few 100 ms by absorption of a small fraction (between 1% and 10%) of the emitted neutrinos. The energy deposition increases the pressure behind the shock, and the respective layers of the star begin to expand. Because of this expansion an extended region of low density, but quite high temperature is created above the surface of the proto-neutron star. The persistent energy input by neutrinos maintains high pressure in this radiation dominated "hot bubble" region, thus driving the shock outward, which eventually causes the supernova explosion. This *delayed explosion mechanism* [5,6] is the currently accepted paradigm (for a review, see, e.g., [7], and for most recent results, see, e.g., [8,9]).

Convective overturn in the neutrino-heated post-shock layer plays an important role during the supernova evolution and can provide the crucial push for the revival of the stalled shock by enhancing the efficiency of neutrino energy transfer [10–12], and the seed for Rayleigh–Taylor instabilities [13]. The latter occur at composition interfaces in the stellar envelope caused by the non-steady propagation of the revived shock and give rise to large scale mixing (see Fig. 2) and clump formation as suggested by observations of SN 1987A (for a review see, e.g., [3]).

From the previous discussion it is obvious that simulating delayed neutrino-driven core collapse supernova explosions is a major computational challenge. Such simulations require a detailed treatment of the neutrino transport particularly inside the semi-transparent hot bubble where the neutrinos deposit their energy, and 2D or better 3D hydrodynamic simulations covering length scales which range (see Fig. 1) from a fraction of the radius of the neutron star ($\sim$15 km) to the radius of the progenitor star ($\sim 3 \times 10^7$ km (3×10^9 km) in case of a blue (red) giant).

The length scale range problem has motivated Kifonidis et al. [13] to perform 2D simulations employing adaptive mesh refinement techniques as implemented in the AMRA code [14]. These up to now unprecedented simulations encompass shock revival by neutrino heating, neutrino-driven convection, explosive nucleosynthesis, the growth of Rayleigh–Taylor instabilities in the stellar envelope at composition interfaces (Fig. 2), and the propagation of newly formed metal clumps through the exploding star. The simulations indicate that for certain progenitors (helium stars), where Kifonidis et al. find a good agreement with observed clump velocities and the amount of mixing, the pattern of clump formation in the ejecta is correlated with the structure of the convective pattern prevailing during the shock-revival phase. This could be used to deduce observational constraints both for the dynamics during the early phase of the evolution, and for the role of neutrino heating in initiating the explosion.

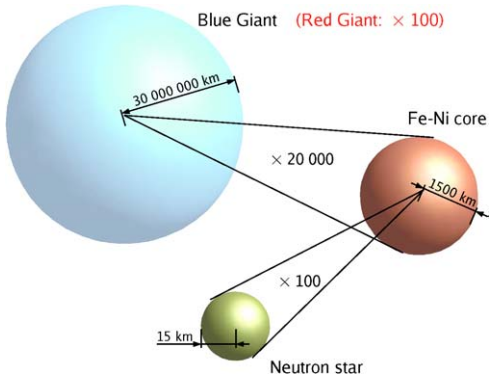

Fig. 1. Length scales involved when modeling a core collapse supernova.

Major difficulties in describing the transport of neutrinos in the semi-transparent regime arise from the strong energy dependence of the neutrino interactions, from non-conservative and anisotropic scattering processes, from the fact that neutrinos are fermions (Fermi blocking), and the need to couple neutrino and anti-neutrino for neutrino-pair reactions. A widely used approximation is multi-energy-group flux-limited diffusion, which, however, is inappropriate for situations where important effects occur in semi-transparent regions. The method is problematic concerning the spectra, luminosities and angular distribution of the neutrinos emitted outside the diffusive regime, as demonstrated by Monte Carlo simulations [15].

As a Monte Carlo treatment of neutrino transport is still far too costly in combination with hydrodynamic

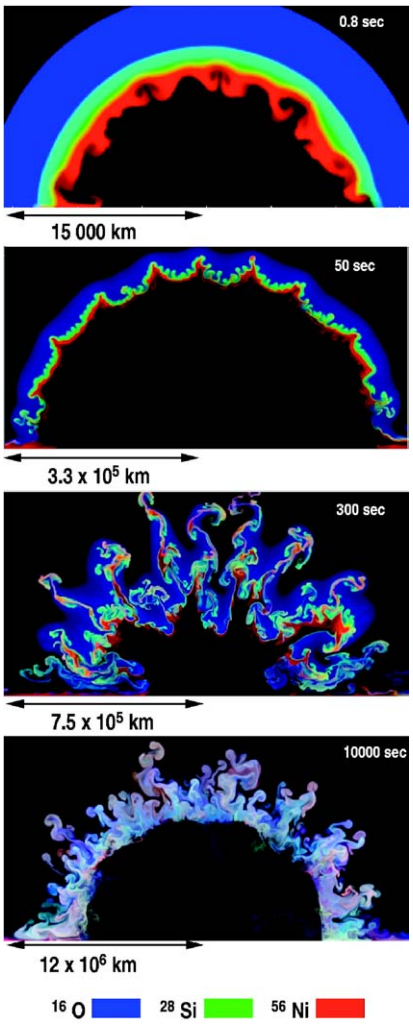

Fig. 2. Compositional mixing in the envelope of a core collapse supernova [13].

simulations, the interest has turned towards other direct solutions of the Boltzmann transport equation. Rampp and Janka [16] have developed an accurate and efficient scheme which solves the discretized energy-dependent moment equations of neutrino number, energy, and momentum of order (v/c) by making use of a variable Eddington factor closure which is calculated from a model Boltzmann equation. One of their simulations requires about 3 months of computation time on a 32 processor node of an IBM Power4 Regatta node. Their treatment of neutrino interactions was recently improved and now includes additional reactions

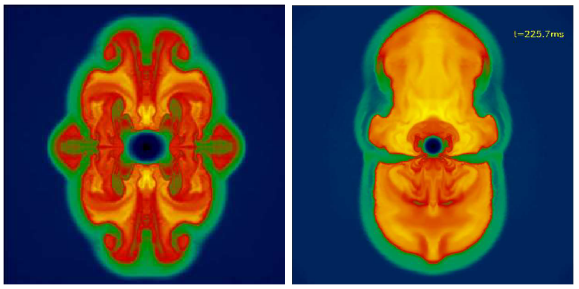

Fig. 3. Snapshots of the entropy distribution for two 2D simulations employing the Boltzmann neutrino transport of [16]. Yellow denotes highest entropies (15–25k_B per nucleon), red, green, and blue ($\lesssim 8k_B$ per nucleon) successively lower values. *Left*: Result at 245 ms post bounce for a $15M_\odot$ progenitor model with a rigidly rotating ($\Omega = 0.5$ rad s^{-1}) iron core [8,17] and assuming equatorial symmetry. At that time the shock reaches its largest expansion of nearly 300 km in the axial (vertical) direction, but later on retreats again. *Right*: Situation in an $11.2M_\odot$ star at 226 ms post bounce [18] when the shock has reached a radius of 600 km with no sign of return. Global, violent low-mode bipolar oscillations of the post-shock layer, which were possible in this simulation as no equatorial symmetry was assumed, support a weak explosion in this *non-rotating* model.

in extension to the standard treatment of neutrino-matter interactions in supernova simulations. Employing their much improved treatment of neutrino transport, they find convective enhancement of shock expansion [8]. However, they are not able to confirm the successful explosions obtained in other simulations involving considerable approximations of the neutrino physics [19–22].

Rotation of the iron core of the progenitor star, even at a moderate rate, supports strong post-shock convection and brings the star much closer to an explosion by the neutrino-heating mechanism. In a simulation of a $15M_\odot$ progenitor where the iron core is assumed to rotate rigidly with a rate of $\Omega = 0.5$ rad s^{-1} [8,17] (which is in the ball park of results from stellar evolution calculations [23] and significantly slower than adopted in other recent investigations [24,25]) the shock expands to a maximum radius of nearly 300 km along the rotation axis (Fig. 3, left). Post-shock convection in the same stellar model, but without rotation, was not strong enough to drive the shock much farther out than in spherically symmetric models [8].

All 2D simulations in Ref. [8], however, were computed using a lateral wedge of about 90°, or assuming in case of the rotating model equatorial symmetry. This restriction constrains the possible modes of the

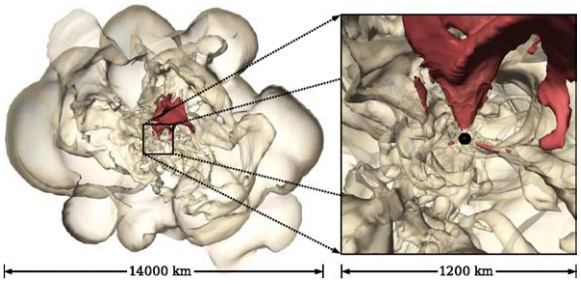

Fig. 4. 3D core collapse simulation [27] one second after bounce. The bright structure is a $Y_e = \text{const.}$ surface which roughly marks the outer boundaries of the neutrino-heated hot bubbles. The dark surface (enlarged in the right panel and defined by a constant value of the mass flux per unit area) marks a downflow of matter towards the neutron star, the surface of which is indicated by the black sphere (corresponding to a density of 10^{11} g/cm^3).

flow pattern in the convective layer. A first 2D simulation with a 180° grid and accurate neutrino transport for a (non-rotating) $11.2M_\odot$ star reveals a dramatic difference compared to the 90° run of this progenitor in Ref. [8]: The shock expands continuously with no sign of return until the simulation was stopped at 226 ms post bounce. At that time the expanding shock is highly deformed and has reached a polar radius of more than 600 km (Fig. 3, right). In the 90° simulation the shock was retreating at that time [8].

The dominance of global dipolar oscillations of the post-shock layer is also seen in 3D simulations neglecting [26] or simplifying [9,27] the treatment of the neutrino transport. The latter work further demonstrates that the merging of modes in three dimensions is as efficient as in two (Fig. 4). The explosion asymmetries also provide a natural explanation for the observed space velocities of neutron stars which on average are in the range of 200–500 km/s a significant fraction moving faster than 1000 km/s (cf. [28]). Scheck et al. [9,27] find neutron star velocities as high as 520 km/s with still large acceleration after the first second, i.e. the final neutron star velocities can therefore be significantly higher.

The non-spherical stratification, mass flow and anisotropic neutrino emission arising from the convective instabilities in the neutrino heated region and from the effects of rotation are, like the ones occurring inside the proto-neutron star, a source of gravitational radiation. Measuring this gravitational wave signal provides unique and direct information about the collapse dynamics. Note in this respect, that the electromagnetic "display" of a core collapse supernova only starts when the shock wave reaches the surface of the progenitor star hours after core bounce. Besides gravitational waves, the only other means to directly probe the collapse dynamics are neutrino observations. A measurement of both the neutrino and the gravitational wave signal would be most exciting, because it would provide extremely important and complementary information for the theoretical modeling of core collapse supernovae. Although such measurements will only be possible for nearby (i.e. galactic) supernovae in the foreseeable future (because of the weakness of the signal), these rare events (one every 20–50 years) would provide a kind of Rosetta stone for supernova research.

As the general relativistic corrections of the gravitational potential during core collapse, and for a neutron star, do not exceed 30%, it is often argued that they can be neglected. While this approach may be justified to some degree in the case of non-rotational core collapse, it becomes very questionable when the core possesses a significant amount of angular momentum, because the stabilizing effect of rotation is counteracted by the destabilizing effect of the deeper relativistic potential. Dimmelmeier et al. [29] performed general relativistic hydrodynamic simulations (using the conformally flat metric approximation to describe the evolution of the time-dependent spacetime metric, and simplified microphysics) of rotational core collapse in axisymmetry and computed the gravitational radiation emitted by such an event. The simulations show that the three different types of gravitational waveforms identified in previous Newtonian simulations are also present in relativistic gravity. For collapse models which are of the same type in both Newtonian and relativistic gravity, the gravitational wave signal is of lower amplitude. If the collapse type differs, weaker as well as stronger signals are found in the relativistic case. For a given model, relativistic gravity can cause a large increase of the characteristic signal frequency of up to a factor of five, which may have important consequences for the signal detection.

3. Simulation of relativistic extragalactic jets

Jets, i.e. highly collimated supersonic outflows, are a common astrophysical phenomenon. They are found

associated with young stellar objects, short-period cataclysmic variables, compact stars and active galactic nuclei (AGNs). In the commonly accepted standard model of extragalactic jets produced by AGNs [30] jet flow velocities as large as 99% (in some cases even beyond) of the speed of light are required to explain the apparent superluminal motion observed at parsec scales in many of these sources. Models which have been proposed to explain the formation of relativistic AGN jets, involve accretion onto a rotating supermassive black hole, which is fed by interstellar gas and gas from tidally disrupted stars through an accretion disk. The observationally inferred relativistic jet velocities suggest that jets are formed within a few gravitational radii of the event horizon of the black hole. Moreover, very-long-baseline interferometric radio observations reveal that jets are already collimated at subparsec scales (see, e.g., [31]). Current theoretical models assume that the accretion disk is the source of the bipolar outflows which are further collimated and accelerated via MHD processes (for a review see, e.g., [32]).

Numerical studies of extragalactic jets can be divided into several distinct categories (for a review see, e.g., [33]). Ordered with increasing distance to the source these categories are the formation and collimation of jets at sub-parsec scales, and the propagation of jets at parsec scales and at kiloparsec scales, respectively. Up to the early 1990s most simulations concerned with the dynamics, morphology and stability of jets were performed in the framework of Newtonian hydrodynamics. This is justified, however, only at distances larger than several kiloparsec (if at all), while at smaller scales a relativistic hydrodynamic modeling is demanded by observations (see above). Simulating the formation and collimation of jets requires both more complicated physics and numerics, because hydromagnetic and general relativistic effects must be considered.

Severe numerical difficulties arise in the integration of the special relativistic hydrodynamic (RHD) equations. The major difficulty is caused by the strong coupling of the equations via the Lorentz factor, which contains all velocity components and appears in all equations. In addition, because there exists no limit to the compression ratio across a shock as the upstream Lorentz factor tends to infinity, relativistic shocks resemble isothermal shocks in Newtonian hydrodynamics producing very thin dense structures, which are difficult to resolve adequately. Only the development of high-resolution shock-capturing finite volume schemes and their application to special relativistic flows has made it possible to overcome the numerical difficulties. There are two main reasons for this success. Firstly, modern schemes do not require any artificial viscosity to handle shocks. Secondly, and even more important, the new methods explicitly take into account the non-linear character of the set of hyperbolic partial differential equations using exact or approximate (relativistic) Riemann solvers. Modern codes (like, e.g., GENESIS [36]) are able to simulate multidimensional relativistic flows with Lorentz factors $\sim 10^3$ (i.e. $v \sim 0.9999995c$) without numerical problems (for a review see, e.g., [33]).

The inclusion of magnetic effects is of great importance for the formation and collimation process of (relativistic) jets which most likely involves dynamically important magnetic fields and occurs in strong gravitational fields. The non-trivial task of developing such a kind of code is considerably simplified by the fact that due to the high conductivity of astrophysical plasmas one must only consider ideal RMHD. The aim of any (Newtonian or relativistic) MHD code is to evolve the induction equation to obtain the magnetic fields from which to calculate the Lorentz force. Magnetic fields are divergence free, i.e. $\nabla \cdot \vec{B} = 0$. Hence, numerical schemes should maintain this constraint (if fulfilled for the initial data) during the evolution, too. This turns out to be no trivial requirement (see, e.g., [37]).

In RMHD one has to solve a non-linear system of conservation laws involving 7 waves (instead of 3 in RHD). The RMHD system is non-strictly hyperbolic (i.e. not all of the real eigenvalues may be distinct), and non-convex (i.e. it possesses characteristic fields which are neither linearly degenerate nor genuinely non-linear). The resulting wave structure is much more complicated than in RHD (compound waves), and involves the additional constraint $\nabla \cdot \vec{B} = 0$. Consequently, the numerical effort is considerably larger than in RHD as more equations, more waves, and degeneracies must be treated. The eigenvalues must be obtained numerically by solving a quartic at each zone interface, because no simple analytic solution in closed form exists. As the eigenvectors depend non-linearly on the eigenvalues, serious numerical complications arise (see, e.g., [37,38]).

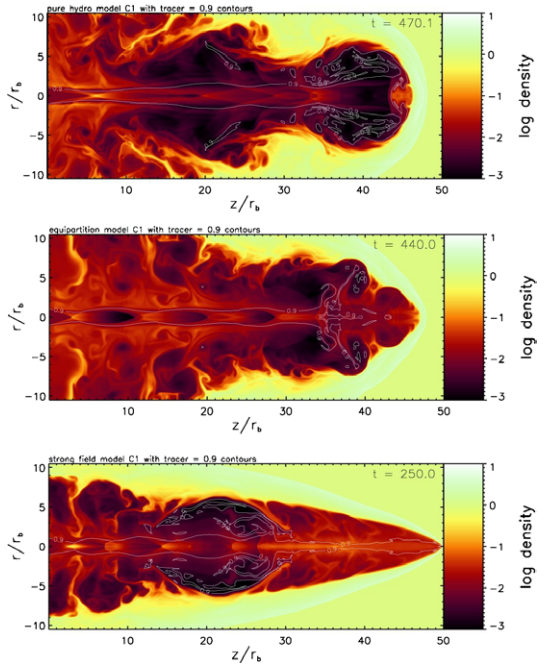

Fig. 5. Influence of the strength of a purely toroidal magnetic field on the morphology of a magnetized relativistic cylindrical jet with a beam velocity of $0.9c$ (model series C1 of [34,35]). The panels show the logarithm of the rest mass density for no magnetic field (top; RHD case), a magnetic field of equipartition strength (middle), and 3.3 times the equipartition strength (bottom). The latter model clearly shows the conspicuous nose cone.

The influence of a (purely) toroidal magnetic field on the morphology of a relativistic cylindrical (2D) extragalactic jet is illustrated in Fig. 5 taken from the comprehensive parameter study of Leismann et al. [34,35]. The most conspicuous feature caused by the toroidal magnetic field is the nose cone at the head of the jet also seen in Newtonian [39] and previous relativistic simulations [40]. This structure forms in jets with toroidal fields of equipartition strength or larger (i.e. magnetic pressure $\gtrsim$ gas pressure), and with a magnetic energy density exceeding a few percent of the rest mass energy.

In order to provide a link between simulation and observation one has to compute observable quantities, e.g., the synchrotron radio emission, from the RHD or RMHD jet simulation data. In case of RHD simulations additional assumptions about the strength and topology of the magnetic field is required, whereas this information is directly available in RMHD models. For example, Aloy et al. [41] have demonstrated that synthetic radio maps from high resolution 3D RHD simulations allow for a study of the observational implications of the interaction between the jet and the external medium. The influence of the matter content of extragalactic jets on their emission properties was studied by Scheck et al. [42] considering jets of extremely different compositions, including pure leptonic and baryonic plasmas. They have computed synthetic radio maps and the thermal bremsstrahlung X-ray emission, and find that the radio emission is dominated by that of the hotspot produced by the terminal shock at the head of the jet. The X-ray surface brightness of their models is suppressed inside the jet cavity, in agreement with recent observations.

4. Simulation of gamma-ray bursts

Gamma-ray bursts (GRBs) are sudden releases of large amounts of energy ($\sim 10^{51}$ erg) in the form of gamma-rays which are, most probably, linked with catastrophic collapse events of massive stars (collapsars [43]) or with mergers of compact binaries [44,45]. In both scenarios a fraction of the gravitational binding energy released by accretion of matter from a thick torus girding a stellar mass black hole (BH) is thought to power a pair fireball. Assuming that the baryon load of the fireball is not too large, the baryons are accelerated together with the e^+e^- pairs to Lorentz factors $>10^2$ (for a review see, e.g., [46]).

Due to their different duration and spectral properties GRBs are commonly divided in two classes: short ($\leqslant 2$ s) and long ($\geqslant 2$ s) GRBs [47]. The long subtype of GRBs has been quite extensively observed, and there is a relatively large number of afterglow multi band observations from radio to X-rays. These observations have shed some light on the kind of progenitors and environments in which such progenitors reside. From the numerical point of view, the generation and early evolution of long GRBs in the framework of the collapsar model has been studied using 2D Newtonian [48] and relativistic hydrodynamics [41,49]. Observations of short GRBs are less numerous and it has not been possible to detect them in multi frequency searches.

The scenario arising after the merging process of a compact binary system consists of a central BH of

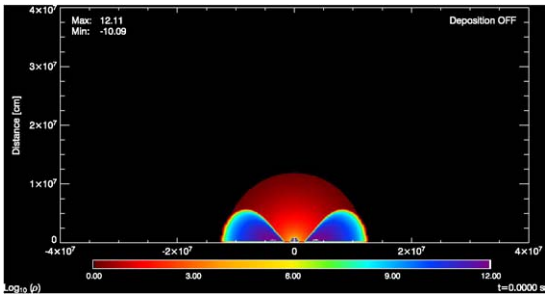

Fig. 6. Logarithm of the rest-mass density of the initial model B01 of [52] showing the structure of the accretion torus.

a few solar masses girded by a thick accretion torus whose mass is of 0.05–0.3$M_\odot$ [50,51]. Once the thick disk is formed, up to $\sim 10^{51}$ erg can be released above the poles of the BH in a region that contains less than $10^{-5} M_\odot$ of baryonic matter due to the release of energy via ν–$\bar{\nu}$ annihilations. This can lead to the acceleration of this matter to ultrarelativistic speeds accounting for a successful GRB [52]. If the duration of the event is related to the lifetime of the system this kind of events can only produce short GRBs because the expected time scale on which the BH engulfs the disk is fractions of a second [50].

That a local deposition of energy around the remnant left over from the merger of two neutron stars can indeed yield the formation of a pair of relativistic, collimated plasma outflows in opposite directions that can account for short GRBs was recently demonstrated by Aloy et al. [52]. These authors present the first general relativistic hydrodynamic models (using the GENESIS code [36]) of the launch and evolution of relativistic jets and winds, driven by thermal energy deposition, possibly due to neutrino–antineutrino annihilation, in the close vicinity of black hole-accretion torus systems (Fig. 6), which are considered to be the remnants of compact object mergers. The simulations establish the link between models of such mergers and future observations of short gamma-ray bursts by the SWIFT satellite. They show that for polar energy deposition rates above some critical value, a sufficiently baryon free merger environment, and by the interaction with the dense accretion torus an ultrarelativistic outflow with Lorentz factors above 100 is collimated into a sharp-edged cone that is embedded laterally by a wind with steeply declining Lorentz factor (Fig. 7). The viability of post-merger black hole–torus systems

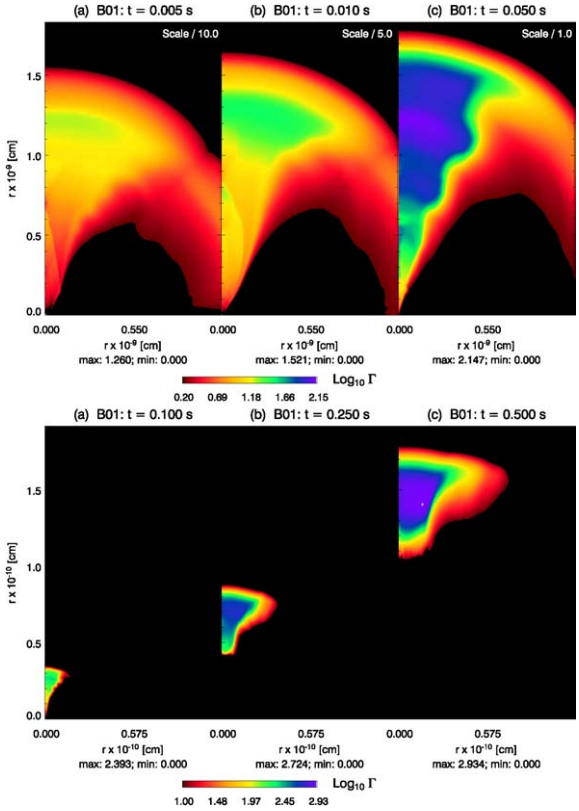

Fig. 7. Snapshots of the logarithm of the Lorentz factor for model B01 of [52] before (top) and after (bottom) shut down of the energy release.

as engines of short, hard gamma-ray bursts is therefore confirmed. Although the torus lifetimes are expected to be only between some 0.01 s and several 0.1 s, the models of Aloy et al. can explain the durations of all observed short gamma-ray bursts, because different propagation velocities of the front and rear ends will lead to a radial stretching of the ultrarelativistic fireball before transparency is reached.

References

[1] W. Baade, F. Zwicky, Phys. Rev. 45 (1934) 138.
[2] F. Hoyle, W. Fowler, Astrophys. J. 132 (1960) 565.
[3] E. Müller, Simulation of astrophysical fluid flow, in: O. Steiner, A. Gautschy (Eds.), Computational Methods for Astrophysical Fluid Flow, Springer, Berlin, 1998, pp. 343–494.
[4] S. Chandrasekhar, An Introduction to the Study of Stellar Structure, Dover, New York, 1939.
[5] H. Bethe, J. Wilson, Astrophys. J. 295 (1985) 14.

[6] J. Wilson, R. Mayle, S. Woosley, T. Weaver, Ann. New York Acad. Sci. 479 (1986) 267.
[7] H.-T. Janka, K. Kifonidis, M. Rampp, Lect. Notes Phys. 578 (2001) 333–363.
[8] R. Buras, M. Rampp, H.-T. Janka, K. Kifonidis, Phys. Rev. Lett. 90 (2003) 241101.
[9] L. Scheck, T. Plewa, H.-T. Janka, K. Kifonidis, Phys. Rev. Lett. 92 (2004) 011103.
[10] M. Herant, W. Benz, W. Hix, C. Fryer, S. Colgate, Astrophys. J. 435 (1994) 339.
[11] A. Burrows, J. Hayes, B.A. Fryxell, Astrophys. J. 450 (1995) 830.
[12] H.-T. Janka, E. Müller, Astron. Astrophys. 306 (1996) 167.
[13] K. Kifonidis, T. Plewa, H.-T. Janka, E. Müller, Astron. Astrophys. 408 (2003) 621.
[14] T. Plewa, E. Müller, Comput. Phys. Comm. 138 (2001) 101.
[15] H.-T. Janka, Astron. Astrophys. 265 (1992) 345.
[16] M. Rammpp, H.-T. Janka, Astron. Astrophys. 396 (2002) 361.
[17] E. Müller, M. Rampp, R. Buras, H.-T. Janka, D. Shoemaker, Astrophys. J. 603 (2004) 221.
[18] H.-T. Janka, R. Buras, K. Kifonidis, A. Marek, M. Rampp, in: Supernovae (10 Years of SN1993J), Proc. IAU Coll. 192, in press; astro-ph/0401461.
[19] C. Fryer, Astrophys. J. 522 (1999) 413.
[20] C. Fryer, A. Heger, Astrophys. J. 541 (2000) 1033.
[21] C. Fryer, M. Warren, Astrophys. J. 574 (2002) L65.
[22] C. Fryer, M. Warren, Astrophys. J. 601 (2004) 391.
[23] A. Heger, S. Woosley, N. Langer, H. Spruit, in: Stellar Rotation, Proc. IAU 215, in press; astro-ph/0301374.
[24] C. Ott, A. Burrows, E. Livne, R. Walder, Astrophys. J. 600 (2004) 834.
[25] K. Kotake, S. Yamada, K. Sato, Astrophys. J. 595 (2003) 304.
[26] J. Blondin, A. Mezzacappa, C. DeMarino, Astrophys. J. 584 (2003) 971.
[27] L. Scheck, Ph.D. thesis, Technical Univ. Munich (2004), submitted for publication (see also astro-ph/0405311 and astro-ph/0408439).
[28] Z. Arzoumanian, D. Chernoff, J. Cordes, Astron. Astrophys. 568 (2002) 289.
[29] H. Dimmelmeier, J. Font, E. Müller, Astron. Astrophys. 393 (2002) 523.
[30] M. Begelman, R. Blandford, M. Rees, Rev. Mod. Phys. 56 (1984) 255.
[31] W. Junor, J. Biretta, M. Livio, Nature 401 (1999) 891.
[32] M. Camenzind, Magnetohydrodynamics of rotating black holes, in: H. Riffert, H. Ruder, H.-P. Nollert, F.W. Hehl (Eds.), Relativistic Astrophysics, Vieweg-Verlag, Braunschweig, Germany, 1998, p. 82.
[33] J. Martí, E. Müller, Numerical hydrodynamics in special relativity, Living Reviews in Relativity, lrr-2003-7.
[34] T. Leismann, Ph.D. thesis, Technical Univ. Munich, 2004, unpublished.
[35] T. Leismann, L. Antón, M. Aloy, E. Müller, J. Martí, J. Miralles, J. Ibáñez, Astron. Astrophys. (2004), in preparation.
[36] M. Aloy, J. Ibáñez, J. Martí, E. Müller, Astrophys. J. (Suppl.) 122 (1999) 151.
[37] G. Tóth, J. Comp. Phys. 161 (2000) 605.
[38] D. Balsara, Astrophys. J. (Suppl.) 132 (2001) 83.
[39] D. Clarke, M. Norman, J. Burns, Astrophys. J. 311 (1986) L63.
[40] S. Komissarov, Mon. Not. Roy. Astron. Soc. 308 (1999) 1069.
[41] M. Aloy, J.-L. Gómez, J. Ibáñez, J. Martí, E. Müller, Astrophys. J. 528 (2000) L85.
[42] L. Scheck, M. Aloy, J. Martí, J.-L. Gómez, E. Müller, Mon. Not. Roy. Astron. Soc. 331 (2002) 615.
[43] S. Woosley, Astrophys. J. 405 (1993) 273.
[44] B. Pacyński, Astrophys. J. 308 (1986) L43.
[45] J. Goodman, Astrophys. J. 308 (1986) L47.
[46] T. Piran, Phys. Rep. 333 (2000) 529.
[47] C. Kouveliotou, C. Meegan, G. Fishman, Astrophys. J. 413 (1993) L101.
[48] A. MacFadyen, S. Woosley, Astrophys. J. 524 (1999) 262.
[49] W. Zhang, S. Woosley, A. MacFadyen, Astrophys. J. 586 (2003) 356.
[50] M. Ruffert, H.-T. Janka, Astron. Astrophys. 344 (1999) 573.
[51] H.-T. Janka, T. Eberl, M. Ruffert, C. Fryer, Astrophys. J. 527 (1999) L39.
[52] M. Aloy, H.-T. Janka, E. Müller, Astrophys. J. (2004), submitted for publication (see also astro-ph/0408291).